EFFECTIVE PROPERTIES FOR PLAIN CONCRETE OBTAINED BY MONO-AXIALLY COMPRESSED CYLINDERS

Elena **Ferretti**

Nota Tecnica N° 54
Bologna – 2001

UNIVERSITÀ DEGLI STUDI DI BOLOGNA – FACOLTÀ DI INGEGNERIA
D.I.S.T.A.R.T. – DIPARTIMENTO DI INGEGNERIA DELLE STRUTTURE,
DEI TRASPORTI, DELLE ACQUE, DEL RILEVAMENTO E DEL TERRITORIO

V.le Risorgimento, 2 – 40136 Bologna

Effective Properties for Plain Concrete Obtained by Mono-Axially Compressed Cylinders

Elena Ferretti*

DISTART – Scienza delle Costruzioni, University of Bologna, Italy, 40136 Bologna (BO)

Abstract

A new procedure is proposed for identifying mono-axial stress-strain relationship and Poisson ratio in compressed plain concrete. By considering the specimen as a structure, the procedure identifies effective properties from experimental data. This way of proceeding involves a modification of traditionally identified mono-axial stress-strain relationship and Poisson ratio. Results are presented for cylinders with varying slenderness.

Keywords: Identification; Concrete; Constitutive law; Poisson ratio; Volumetric curve

1. Introduction

In order to derive a constitutive law in uniaxial compression from experimental data, it is common practice to define the average stress $\bar{\sigma}$ and the average strain $\bar{\varepsilon}$ as shown in Fig. 1. The $\bar{\sigma}$ - $\bar{\varepsilon}$ relationship in Fig. 1 is known as uniaxial constitutive law for monotone strain processes. The term "constitutive" is associated with the $\bar{\sigma}$ - $\bar{\varepsilon}$ relationship since this relationship is considered as representative of the mechanic behaviour of the material. However, one can make the following remarks concerning the choice of this term:

1. The $\bar{\sigma}$ - $\bar{\varepsilon}$ law in Fig. 1 is size-effect sensitive, while a constitutive law should not exhibit a size effect.
2. The identification procedure in Fig. 1 consists of a mere change of scale. Thus, experimental and identified curves are homothetic (Fig. 1). In particular, they both exhibit a softening behaviour. Nevertheless, it is not possible to associate a physical meaning with the softening behaviour of a material response, as the concept of

* Corresponding author. Tel.: +39-51-2093493; fax: +39-51-2093495.
E-mail address: elena.ferretti@mail.ing.unibo.it (E. Ferretti)

instability loses its sense in the infinitesimal neighbourhood of a point [3]. Besides, from the beginning of the 20th century forth, strain-softening has been widely regarded as inadmissible by several authors [4].

These inconsistencies come from the impossibility of performing mechanical tests on the material directly: the object in testing is never the material, but a specimen, that is to say, a structure interacting with the test-machine (Fig. 1, [1]). Thus, experimental results univocally characterise the behaviour of the specimen-test machine system, while they are not at all representative of the constitutive behaviour of the material. In particular, by associating the N-ΔH load-displacement diagram in Fig. 1 with the result of a compressive test on aggregative material, the softening branch has a meaning that is only linked to the structural instability. This branch cannot provide information on the material constitutive behaviour, but through an identifying model. That is to say, to identify constitutive laws starting from experimental results it is necessary to evaluate all factors influencing a test result. Indeed, since the specimen is a structure, experimental results (R) depend not only on constitutive properties (C), but also on structural mechanics (S), interactions between test-machine and specimen (I), and test-machine metrological characteristics (M):

$$R = C + S + I + M \ . \tag{1}$$

On the base of partially analogous considerations, Rosati et. al. [2] have recently proposed a complete response for concrete loaded in tension.

It is then necessary to define an identifying procedure from experimental data to material behaviour (inverse problem), which is not affected by the remarks concerning the approach in Fig. 1. In the present paper, a proposal for the identification of the effective stress-effective strain relationship of concrete in monotone uniaxial compression is presented.

2. Identification approach of σ-ε effective behaviour in mono-axial compression

2.1. Identification of the effective stress

Name K_C, K_S, K_I, and K_M the weighed contributions assumed by *C*, *S*, *I*, and *M*, respectively, in the definition of *R* (Eq. (1)):

$$C = K_C R\,, \quad S = K_S R\,, \quad I = K_I R\,, \quad M = K_M R\,. \tag{2}$$

With this position, it follows that $K_C + K_S + K_I + K_M = 1$.

All the contributions but the constitutive behaviour can be grouped in one factor:

$$K = K_S + K_I + K_M\,. \tag{3}$$

From the identifying procedure in Fig. 1 it follows that:

$$C \equiv R\,. \tag{4}$$

With the position in Eq. (3), the Eq.(4) is replaced by the relationship:

$$C = (1 - K)R\,. \tag{5}$$

The equation (5) allows evaluation of the constitutive properties, taking into account the behaviour of the specimen-test machine system, which is represented by the parameter *K*. This approach is formally more correct that the approach in Eq. (4). Nevertheless, it is not of immediate use for identifying constitutive properties, since $K_C = K_C(R)$, $K_S = K_S(R)$, $K_I = K_I(R)$, and $K_M = K_M(R)$ are, generally speaking, load-step functions. That is to say,

$$K = K(R) \tag{6}$$

is a load-step function, and not a constant of the performing test.

In conclusion, it is not possible to establish a homothetic correspondence between the experimental load-displacement relationship and the uniaxial constitutive stress-strain relationship. Moreover, since Eq. (6) is not of objective determination, *K* can only be estimated, with regard to the material scale. This involves the identification of an effective response, and not of a constitutive response in its rigorous meaning.

The main consequence of Eqs. (5) and (6) is the loss of the traditional identity between the experimental and the effective curve shape. In other words, the effective curve may not exhibit the typical softening behaviour of the experimental curve. Since it is impossible to associate a physical meaning with the strain-softening behaviour of a material response, it can be asserted that the identified effective laws must be monotone nondecreasing for any material.

An analysis of the reciprocal ratios between K_C, K_S, K_I, and K_M for compressed concrete cylinders [3] showed that it is possible to assume $K \cong K_S$. Thus, the large structural scheme variation following from the propagation of dominant bi-cone shaped cracks is preponderant in comparison to the other addends in Eq. (3). To identify the scale factor of the σ axis with respect to the *N* axis (Fig. 1), it is fundamental to introduce a parameter whose dimensions are those of an area and whose incremental law is linked to the structural scheme variation. In the following, this parameter will be termed the resistant area A_{res}. In the assumption that $K \cong K_S$, any specimen can be regarded as composed by a resistant structure (Fig. 2), in which crack propagation never occurred, and a volume of incoherent material.

In this study, it was proposed to estimate the resistant area A_{res} in accordance with the Fracture Mechanics with Damage:

$$A_{res} = A_n\left(1 - D\right), \tag{7}$$

where *D* is a scalar.

In accordance with Eq. (7), the effective stress has been defined as the average stress acting on the area A_{res}:

$$\sigma_{eff} = \frac{N}{A_{res}}. \tag{8}$$

Alternatively, the effective stress can be expressed as:

$$\sigma_{eff} = \overline{\sigma}\frac{A_n}{A_{res}}. \tag{9}$$

The analogy with the manner of operation of the Fracture Mechanics with Damage is limited to Eq. (7). Indeed, in the Fracture Mechanics with Damage, *D* has an analytic

formulation and is considered as uniformly distributed on A_n. In this study, $D = D(R)$ is experimentally evaluated and is considered as localised in the volume of incoherent material.

2.1.1. Algebraic considerations about the formulation of the effective stress

In this paragraph, an interesting information about the sign of the effective stress derivative in the σ_{eff} - $\bar{\varepsilon}$ plane is provided. In the following, it will be shown how this information directly rises from the formulation of the effective stress in Eq. (8), in which A_{res} is computed in accordance with Eq. (7). Put Eq. (8) in the form:

$$\sigma_{eff}(v) = \frac{N(v)}{A_{res}(v)}, \tag{10}$$

where the dependence of σ_{eff}, A_{res}, N e D on the displacement v is explicit. Now, find the derivative of Eq. (10) with respect to the variable $\bar{\varepsilon}$:

$$\frac{d\sigma_{eff}}{d\bar{\varepsilon}} = \sigma'_{eff}\frac{dv}{d\bar{\varepsilon}} = H\frac{N'A_{res} - NA'_{res}}{A_{res}^2}. \tag{11}$$

The superscript indicates derivation with respect to the variable v, and H is the gage length of $\bar{\varepsilon}$:

$$v = H\bar{\varepsilon}. \tag{12}$$

For the conventions in Fig. 1, it follows that:

$$N(v)\big|_{v=\hat{v}} = N_{\max}, \tag{13}$$

where $\hat{v}$ is the value of impressed displacement corresponding to the maximal load. As to the discussion of the sign of Eq. (11), it can be stated that:

- N is a monotone nondecreasing function until the peak ($N' \geq 0$, $0 \leq v \leq \hat{v}$), and a monotone strictly nonincreasing function beyond the peak ($N' < 0$, $v > \hat{v}$);
- A_{res} is a monotone nonincreasing function on all the domain ($A'_{res} \leq 0$, $\forall v$), and it can assume a zero tangent only in a neighbourhood of the origin, corresponding to the linear elastic state of the material.

For Eq. (7), the assumption of monotonicity for A_{res} involves a condition of monotonicity for the damage law.

The experimental results agree with the condition of non zero tangent of A_{res} and D for $v = \hat{v}$, since the crack propagation rate near $v = \hat{v}$ is always very fast:

$$A'_{res}\big|_{v=\hat{v}} \neq 0 , \qquad D'\big|_{v=\hat{v}} \neq 0 . \tag{14}$$

From the above discussion, it follows immediately that the sign of $d\sigma_{eff} / d\bar{\varepsilon}$ is positive for $0 \leq v \leq \hat{v}$:

$$\frac{d\sigma_{eff}}{d\bar{\varepsilon}} > 0 \qquad 0 \leq v \leq \hat{v} . \tag{15}$$

In particular, for $v = \hat{v}$ the Eq. (11) assumes the value of:

$$\left.\frac{d\sigma_{eff}}{d\bar{\varepsilon}}\right|_{v=\hat{v}} = -NH \frac{A'_{res}}{A^2_{res}} > 0 , \tag{16}$$

in which the strict inequality comes from Eq. (14).

From Eq. (15), the first result of fundamental importance follows: a point with strictly positive tangent in the σ_{eff} - $\bar{\varepsilon}$ curve corresponds to the point with zero tangent in the *N*-*v* curve. This is a notable result, since it has been obtained without having introduced any other assumptions on the shape of the damage law except the physically justifiable condition of non zero tangent in correspondence of the maximal load. It can easily be demonstrated how the same result for the sign of the tangent can be transposed to the σ_{eff} - ε_{eff} curve, in the point corresponding to the $v = \hat{v}$ point of the *N*-*v* curve.

As regards the sign of Eq. (11) for $v > \hat{v}$, this depends on the value of ρ, the ratio between the two terms in the numerator of Eq. (11):

$$\rho = \frac{N' A_{res}}{N A'_{res}} . \tag{17}$$

The result is:

$$\frac{d\sigma_{eff}}{d\bar{\varepsilon}} \geq 0 \qquad \forall v > \hat{v} , \; 0 \leq \rho \leq 1 \tag{18′}$$

$$\frac{d\sigma_{eff}}{d\bar{\varepsilon}} < 0 \qquad \forall v > \hat{v}\,,\ \rho > 1\,. \tag{18''}$$

In alternative to Eqs. (18), one can study the sign for $v > \hat{v}$ of the derivative of *q*, defined as follows:

$$q = \frac{\bar{\sigma}_{\max}}{\sigma_{eff}} \overset{(7)}{=} \frac{A_{res}}{A_n} \Big/ \frac{N}{N_{\max}}\,, \tag{19}$$

in which the function *q* has been expressed as the ratio between the normalised resistant area and the normalised load. It follows that:

$$q' = -\bar{\sigma}_{\max} \frac{\sigma'_{eff}}{\sigma^2_{eff}} = -\bar{\sigma}_{\max} \frac{N'A_{res} - NA'_{res}}{N^2}\,. \tag{20}$$

From Eq. (20) it can be observed that the sign of q' too is determined by the ratio ρ. The result is:

$$q' > 0 \qquad \forall v > \hat{v}\,,\ \rho > 1\,; \tag{21'}$$

$$q' \le 0 \qquad \forall v > \hat{v}\,,\ 0 \le \rho \le 1\,. \tag{21''}$$

On the other hand, the sign of q' follows directly from Eqs. (18) and the first equality in Eq. (20), which states that the signs of q' and σ'_{eff} are unconformable $\forall v$.

In conclusion, the sign of $d\sigma_{eff}/d\bar{\varepsilon}$ is surely positive for $0 \le v \le \hat{v}$, whereas it is only known when the damage law is known for $v > \hat{v}$. Also this result can easily be transposed to the sign of the derivative of the σ_{eff} - ε_{eff} curve.

2.2. Identification of the effective strain

As regards the scale factor of the ε axis with respect to the *v* axis (Fig. 1), the effective strain ε_{eff} has been identified considering that only the conservative forces act in a generic unloading-reloading cycle. In other words, these cycles should be characterised by constant values of resistant area. For this assumption, the instantaneous secant stiffness of the σ_{eff} - ε_{eff} law, $E_s = \tan\alpha$ (Fig. 3), is taken equal to the average slope of

the unloading-reloading cycle at the current point. Thus, the generic point σ_{eff} - ε_{eff} results from the intersection of the two lines $\sigma = \sigma_{eff}$ and $\sigma = E_s \varepsilon$.

Fig. 3 shows the identification of the effective strain ε_{eff}, starting from the value of effective stress σ_{eff} (Eqs. 8 and 7) and the knowledge of the damage law *D*.

3. Results for the concrete in monotone uniaxial compression

To operate the transformation in Fig. 3 from the $\overline{\sigma}$ - $\overline{\varepsilon}$ diagram to the σ_{eff} - ε_{eff} diagram, the damage law *D* and the unloading law must be known. In the following, a proposal to experimentally evaluate these laws is presented.

The results shown in the following sections belong to an experimental programme [3] on cylindrical concrete specimens. In this programme, six geometries of specimens have been taken into account, with the height-radius ratio variable between three and eight. Three specimens have been made for each of the six geometries. All the eighteen specimens have been tested in monotone uniaxial load, in the same thermo-hygrometric and curing conditions.

3.1. Unloading law

The Fig. 4 shows how the unloading law is sensibly independent on the slenderness of the specimens. This result supports the assumption for which all the parameters characterising the unloading-reloading cycles, included their average slope, are linked to proprieties of the material and do not depend on the structural mechanics. This happens since the resistant area does not change in the unloading-reloading cycles.

3.2. Experimental damage law

To evaluate $D = D(R)$, two experimental damage laws were employed. The first damage law, D_1 [5], relates the damage to the percentage variation of the microseismic signal velocity *V* at the current point (set-up of the microseismic test in Fig. 5.a):

$$D_1 = 1 - V/V_0 \,, \tag{22}$$

where V_0 is the initial microseismic signal velocity.

The second damage law, D_2 [6], relates the damage to the dissipated energy W_d at the current point (Fig. 5.b):

$$D_2 = W_d / W_{d,t} \ , \tag{23}$$

where $W_{d,t}$ is the total dissipated energy. The evaluation of W_d has been done in accordance with the experimental unloading law.

D_1 and D_2 turned out to be very close to each other [3], until the acceptability threshold of the added noise. This threshold corresponds to the value of deformation beyond which the noise of the crack propagation disturbs the microseismic survey so much that the variations of the microseismic signal cannot be appreciated any longer. For Eq. (7), the D_1 and D_2 experimental damage laws can be seen in Fig. 6 as the one's complement of the corresponding percentage resistant area laws.

To identify the effective properties, only the D_2 damage law has been used in the following, since this law is not affected by limitations in the survey field.

The assumption of only conservative forces acting on the unloading-reloading cycles allows evaluation of the specimen defects at the natural state, through the amount of initial damage D_0 [6]. Indeed, for the mentioned assumption, D_0 comes from the ratio between the slope of the stabilising cycle and the tangent to the origin of the *N*-*v* diagram (Fig. 7):

$$D_0 = 1 - \frac{E^0(\varepsilon)}{E^0_{eff_1}(\varepsilon)} \cong 1 - \frac{\tan\phi_c^0}{\tan\phi_s} \, . \tag{24}$$

It must be incidentally recalled that a stabilising cycle is an unloading-reloading cycle that is effectuated for a preloading equal to about the 10% of the maximal presumed load. The stabilising cycle is done in order to limit the influence of the specimen-test machine interaction and test-machine metrological properties on the experimental result. The moderate value of the preloading and the mechanical meaning of the unloading-reloading slopes allow one to associate the difference between the loading and unloading slopes with a damage that is load history independent. This damage characterises the specimen at the natural state.

In accordance with Eq. (24), Eq. (7) has been modified as follows:

$$A_{res} = A_n\left(1 - D_{eq}\right). \tag{25}$$

D_{eq} is the equivalent damage, comprehensive both of the initial damage D_0 and the damage D_2 due to the monotone loading. D_{eq} can be expressed as:

$$D_{eq} = 1 - \left(1 - D_0\right)\left(1 - D_2\right) = D_0 + D_2 - D_0 D_2 . \tag{26}$$

The nominal area deprived of the defects at the natural state, termed the reduced nominal area A_n', results from:

$$A_n' = A_n\left(1 - D_0\right). \tag{27}$$

Damage laws were experimentally derived for variable specimen slenderness. The Fig. 8 shows the D_2 damage laws obtained for H/R ratios varying from 3 and 8. As can be seen in Fig. 8, damage laws are size-effect sensitive. That is, the highest is the H/R ratio, the highest is *D* for every load-step.

3.3. Sign of the effective stress derivative

As previously stated, the experimental damage law can be seen in Fig. 9 as the one's complement of the percentage resistant area law. The derivative of the experimental damage law in Fig. 9, D', turned out to be very close to assume a maximum for $v = \hat{v}$. This result represents the experimental validation of the assumption in Eq. (14), and, as already stated, corresponds to a fast crack propagation situation.

The discussion on D' is independent on the single test, and the behaviour in Fig. 9 for $v = \hat{v}$ can be generalised. Indeed, the adopted damage law (Eq. (23)) has a shape that is widely determined by the integral of the *N*-*v* curve. Hence, since the *N*-*v* curve exhibits a maximum for $v = \hat{v}$, the damage law assumes its maximum derivative in the neighbourhood of $\hat{v}$.

As regards the sign of the effective stress derivative after the peak, the experimental $q(v)$ function turned out to be a positive-valued, monotone strictly nonincreasing function (Fig. 10):

$$q'(v) < 0 \qquad \forall v . \tag{28}$$

This implies that the resistant area decreasing rate was faster than the load decreasing rate. This circumstance and the negative sign between q' and σ'_{eff} (Eq. (20)) ensure the effective stress derivative to be positive also for $v > \hat{v}$.

In conclusion, for the performed experimental programme and the damage law in Eq. (23), the effective stress derivative always assumes a finite positive value:

$$\frac{d\sigma_{eff}}{d\bar{\varepsilon}} > 0 \qquad \forall v . \tag{29}$$

3.4. Effective curve

The *N*-*v* diagrams for the six specimens with varying slenderness of the experimental programme [3] are shown in Fig. 11. In this Figure, the size-effect in the *N*-*v* plane involves both a decrement of the tangent to the origin with the increasing of the $H - R$ ratio, and a decrement of the maximum load with the increasing of the $H - R$ ratio.

The σ_{eff} - ε_{eff} relationships obtained for the six tested geometries fall within the grey region in Fig. 12 (dispersion range). As previously stated, a strictly positive derivative for the effective properties curves in the σ_{eff} - ε_{eff} plane directly follows from the independence of the behaviour in Fig. 9 on the single test. Moreover, it can be stated that the effective properties curves are size-effect insensitive, since the dispersion range is very little.

The average curve shape in the σ_{eff} - ε_{eff} plane is representative of the meso-scale material behaviour.

4. Identification of the Poisson ratio

With reference to the traditional approach, said $\varepsilon_r = \Delta R / R$ the radial strain and $\varepsilon_l = \Delta H / H$ the longitudinal strain for a uni-axially compressed solid, the Poisson ratio is defined as $\nu = -\varepsilon_r / \varepsilon_l$. If ε_l is of immediate determination, things are different for ε_r, since it is not easy to measure a radial strain. A way to solve this problem is to reduce the radial measure to a circumferential measure:

$$\varepsilon_r = \frac{\Delta R}{R} = \frac{2\pi\Delta R}{2\pi R} = \frac{\Delta crf}{crf}. \tag{30}$$

Operatively, radial strain can be acquired by means of a circumferential strain gauge [1, [3], maintained in the right position using a chain (Fig. 13). Nevertheless, strain measurements acquired on cylindrical specimen surface cannot be employed to evaluate the Poisson ratio, because they are affected by crack openings. Even this time, the model traditionally assumed to identify a constitutive property is not accurate enough to interpret the physical problem. The resultant $\varepsilon_r/\varepsilon_l$ ratio in function of ε_l is a monotone nondecreasing relationship [7] (Fig. 13).

To avoid the acquisition of crack openings, fibre optic sensors (FOSs) have been utilised [3] to acquire radial strains internally to the resistant structure (Fig. 13). The $\varepsilon_r/\varepsilon_l$ ratio for this new acquisition is almost constant with ε_l (Fig. 13).

Since in this study it was assumed that macro-cracks do not occur in the resistant structure, the new constant behaviour of $\varepsilon_r/\varepsilon_l$ could be considered more representative of the Poisson ratio ν than the traditional increasing behaviour of $\varepsilon_r/\varepsilon_l$ is. To evaluate the actual Poisson ratio, the actual stress state in the resistant structure must be taken into account, since this state is tri-axial in any case.

Finally, the new volumetric curve integrally belongs to the negative field, while the traditional volumetric curve also develops in the positive filed [7] (Fig. 14). Thus, on the contrary of what traditionally asserted [7], it is possible to assume that the concrete never exhibits a dilatant behaviour.

5. Conclusions

A concrete specimen under uniaxial monotone compression in displacement-control is characterised by a load (N)-displacement (v) diagram with softening. During the loading, the specimen exhibits a crack propagation pattern that depends on the structural mechanics and the interaction with the test-machine. The N-v diagram itself is affected by the structural mechanics and the interaction between the specimen and the test-machine, since the crack propagation modifies the resistant structure.

The aim of this study was to identify the mechanical properties of the material, starting from the experimental behaviour of the whole specimen-test machine system (*N*-*v* diagrams). These identified mechanical properties have been termed the "effective properties".

Considering the specimen as a structure interacting with the test-machine, it was demonstrated that the σ_{eff} - ε_{eff} curve of damaging materials exhibits a strictly positive derivative at the point corresponding to the peak of the $\overline{\sigma}$ - $\overline{\varepsilon}$ curve. This result is independent on the adopted damage law.

An experimental programme on cylindrical concrete specimens in uniaxial compression has been performed. A procedure to experimentally evaluate the damage law has been proposed. The adopted damage law led to monotone strictly nondecreasing σ_{eff} - ε_{eff} curves for all concrete specimens. Moreover, this curve turns out to be size-effect insensitive. The proposed approach allows identification of a σ_{eff} - ε_{eff} relationship for the description of the meso-scale material behaviour. This relationship, together with adequate failure criteria, leads to structural analysis [3].

By means of strain acquisitions internally to the resistant structure, a very close Poisson ratio was estimated to be constant with the longitudinal strain [1]. From the constant value of the Poisson ratio, it follows that concrete never exhibits a dilatant behaviour [1]. What we know as dilatant behaviour of the concrete [7] comes from an erroneous acquisition of radial strain, which is affected by crack openings.

The qualitative evaluations of the Poisson ratio and of the specific variation of volume, from strain measurements acquired inside the resistant structure, can provide useful information for the description of the effective response in tri-axial state.

Acknowledgements

This study has been carried out with the financial support of the Italian Ministry for Universities and Scientific and Technological Research (MURST).

Profs. Erasmo Viola and Antonio Di Leo are gratefully acknowledged for their suggestions and scientific supervision.

References

[1] Ferretti E, Carli R. Programma Sperimentale sul Comportamento in Compressione Monoassiale del Calcestruzzo; Parte II: Elaborazione dei Risultati Sperimentali. Technical note 33, DISTART – University of Bologna – Italy, 1999 (in Italian).

[2] Rosati G, Natali Sora MP. Direct Tensile Tests on Concretelike Materials: Structural and Constitutive Behaviors. J. Engng Mech. 2001;127:364-371.

[3] Ferretti E. Modellazione del Comportamento del Cilindro Fasciato in Compressione. Ph.D. Thesis: University of Lecce – Italy, 2001 (in Italian).

[4] Bažant ZP, Belytschko TB, Chang T. Continuum Theory for Strain-Softening. J. Engng. Mech. 1984;110(12):1666-1692.

[5] Daponte P, Olivito RS. Crack Detection Measurements in Concrete. Proceedings of the ISMM International Conference Microcomputers Applications, December 14-16, 1989, pp.123-127.

[6] Ferretti E, Viola E, Di Leo A, Pascale G. Propagazione della Frattura e Comportamento Macroscopico in Compressione del Calcestruzzo. XIV AIMETA, October 1999 (in Italian).

[7] Di Leo A, Di Tommaso A, Merlari R. Danneggiamento per Microfessurazione di Malte di Cemento e Calcestruzzi Sottoposti a Carichi Ripetuti. Technical Note 46, DISTART – University of Bologna – Italy, 1979 (in Italian).

Figure captions

Fig. 1. Traditional identification of mono-axial constitutive law by experimental tests.

Fig. 2. Resistant structure at the end of the test.

Fig. 3. Identification of ε_{eff} starting from the known value of σ_{eff} .

Fig. 4. Interpolating law of the unloading-reloading cycles average slope variation for variable slenderness.

Fig. 5. a) Test set-up for the acquisition of D_1 ; b) Evaluation of W_d for the acquisition of D_2 .

Fig. 6. Comparison between the energetic and microseismic laws.

Fig. 7. Parameters used to evaluate initial damage D_0 .

Fig. 8. Evolution of resistant area and D_2 damage law for variable slenderness.

Fig. 9. Comparison between the load and resistant area normalised laws.

Fig. 10. Scale factor between the percentage resistant area and normalised load laws.

Fig. 11. Size effect for the load-displacement diagrams.

Fig. 12. $\sigma_{eff} / \varepsilon_{eff}$ dispersion range for variable slenderness and average curve.

Fig. 13. Traditional and identified $\varepsilon_r / \varepsilon_l$ ratios.

Fig. 14. Traditional and identified volumetric curves.

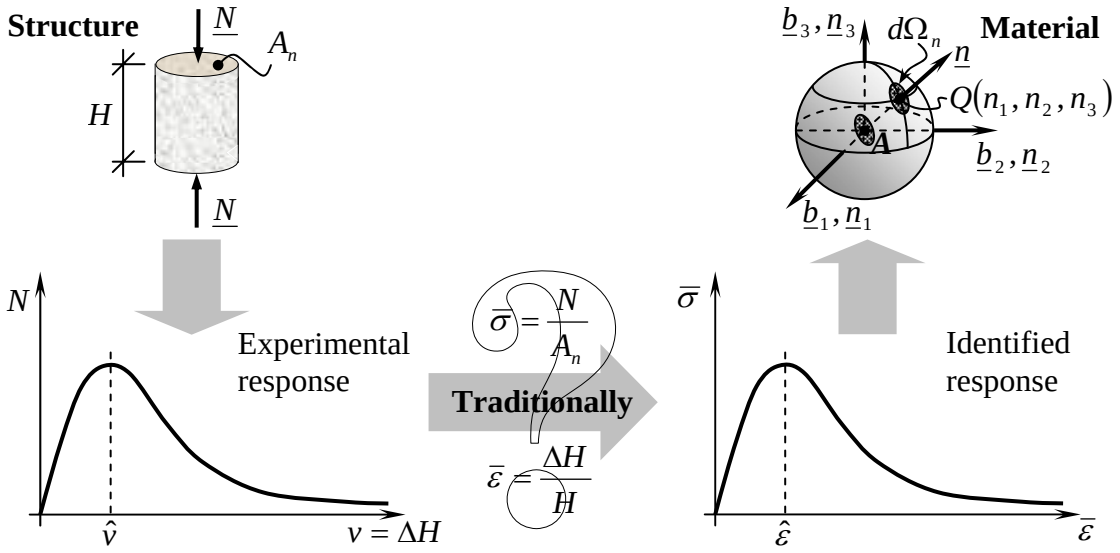
Structure
N
A_n
H
N
N
ν = ΔH
ν̂
Experimental response
σ̄ = N / A_n
Traditionally
ε̄ = ΔH / H
b_3, n_3
dΩ_n
n
Q(n_1, n_2, n_3)
A
b_2, n_2
b_1, n_1
Material
σ̄
ε̄
ε̂
Identified response

Fig. 1 – Elena Ferretti

Fig. 2 – Elena Ferretti

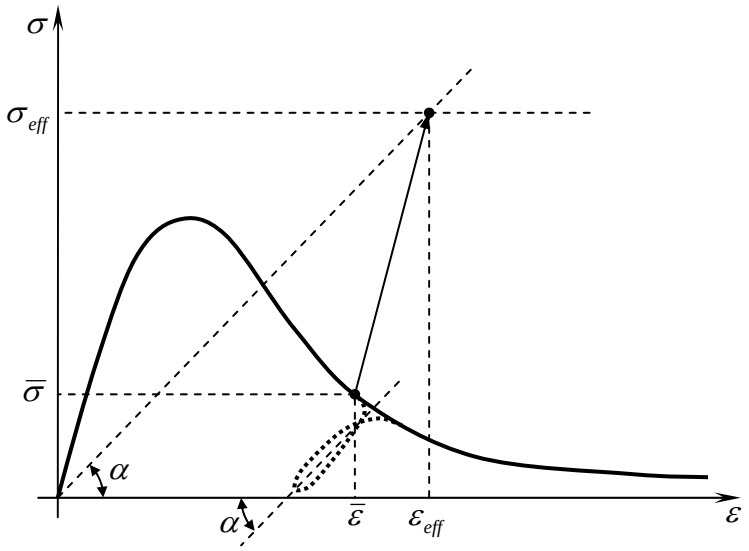
σ
σ_eff
σ̄
α
α
ε̄
ε_eff
ε

Fig. 3 – Elena Ferretti

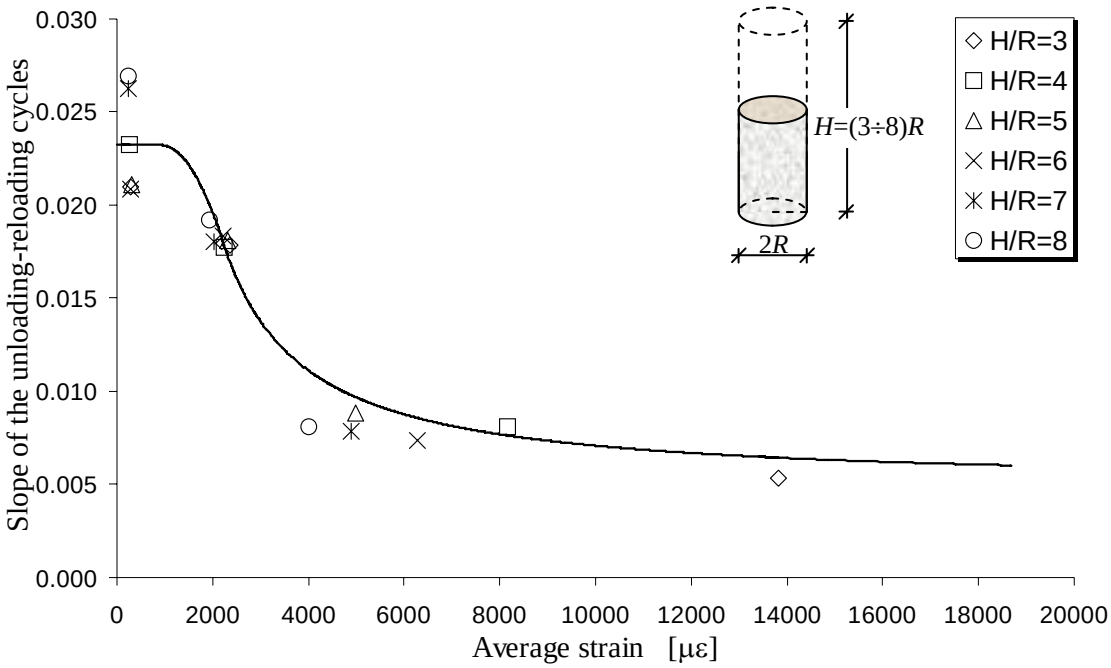
0.030
0.025
0.020
0.015
0.010
0.005
0.000
Slope of the unloading-reloading cycles
0
2000
4000
6000
8000
10000
12000
14000
16000
18000
20000
Average strain [με]
H=(3÷8)R
2R
H/R=3
H/R=4
H/R=5
H/R=6
H/R=7
H/R=8

Fig. 4 – Elena Ferretti

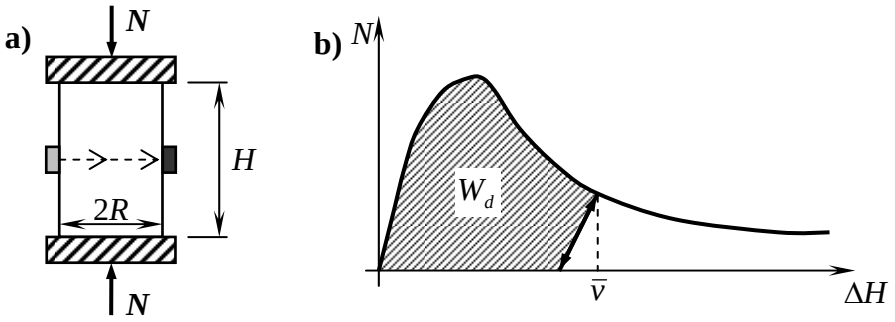
a)
N
H
2R
N
b)
N
W_d
$\bar{v}$
ΔH

Fig. 5 – Elena Ferretti

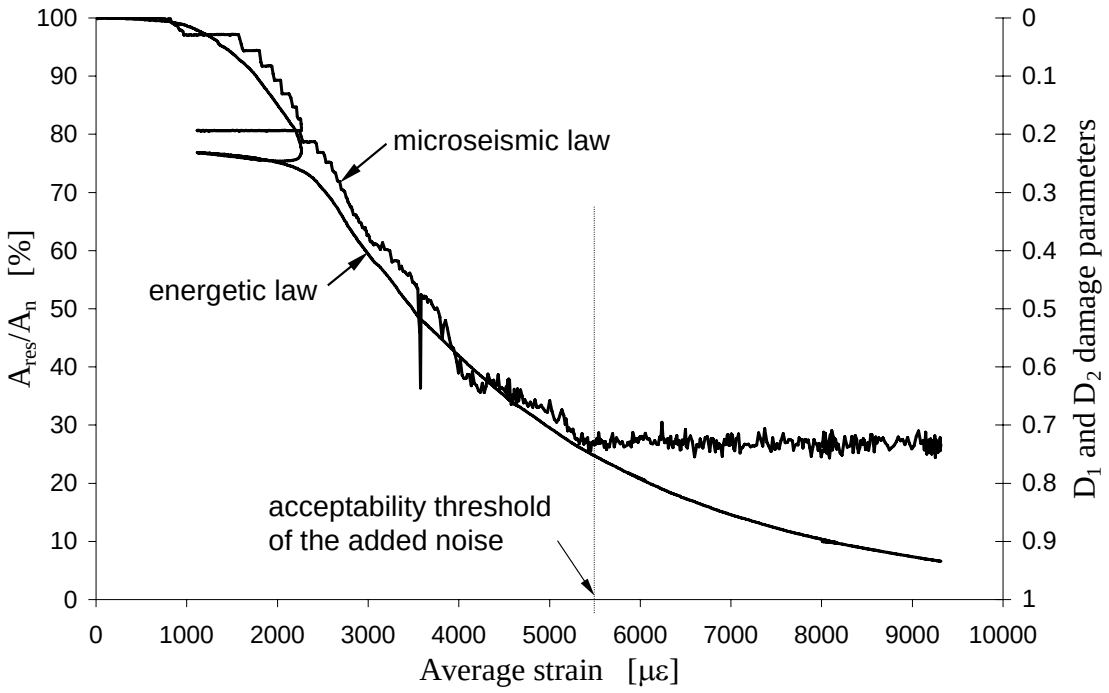
microseismic law
energetic law
acceptability threshold
of the added noise
A_{res}/A_n [%]
D_1 and D_2 damage parameters
Average strain [με]
100
90
80
70
60
50
40
30
20
10
0
0
0.1
0.2
0.3
0.4
0.5
0.6
0.7
0.8
0.9
1
0
1000
2000
3000
4000
5000
6000
7000
8000
9000
10000

Fig. 6 – Elena Ferretti

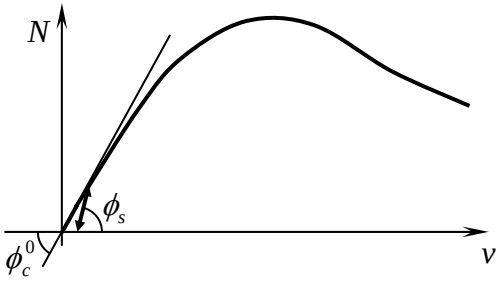
N
ϕ_s
ϕ_c^0
v

Fig. 7 – Elena Ferretti

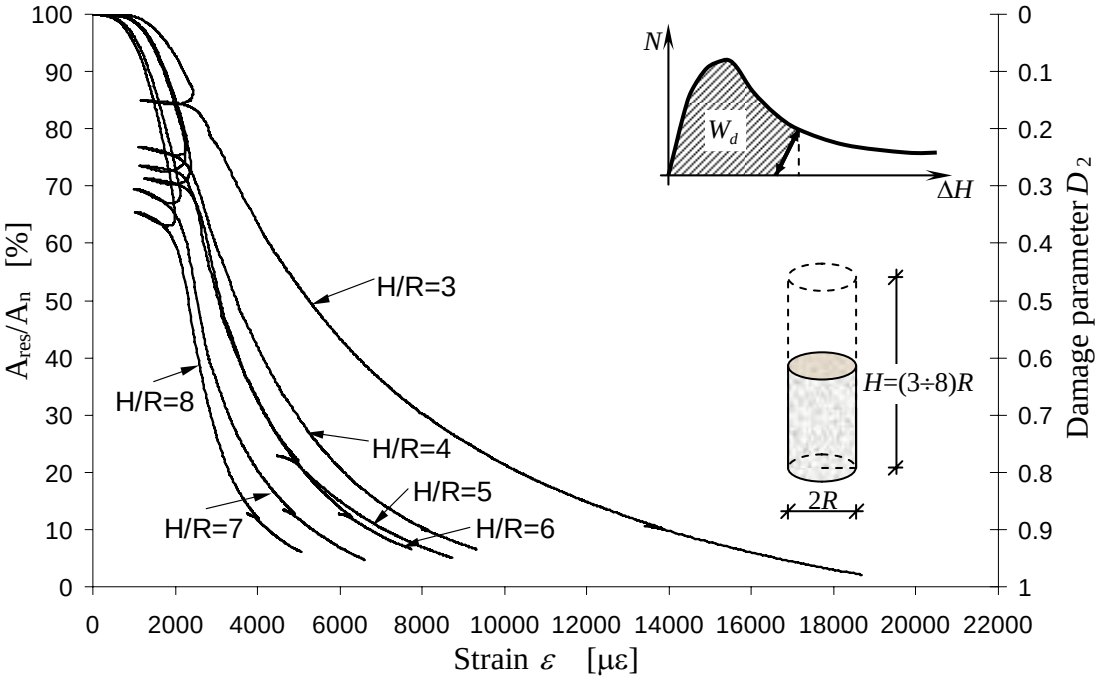
100
90
80
70
60
50
40
30
20
10
0
0
2000
4000
6000
8000
10000
12000
14000
16000
18000
20000
22000
Strain ε [με]
Ares/An [%]
Damage parameter D2
0
0.1
0.2
0.3
0.4
0.5
0.6
0.7
0.8
0.9
1
H/R=3
H/R=4
H/R=5
H/R=6
H/R=7
H/R=8
N
Wd
ΔH
H=(3÷8)R
2R

Fig. 8 – Elena Ferretti

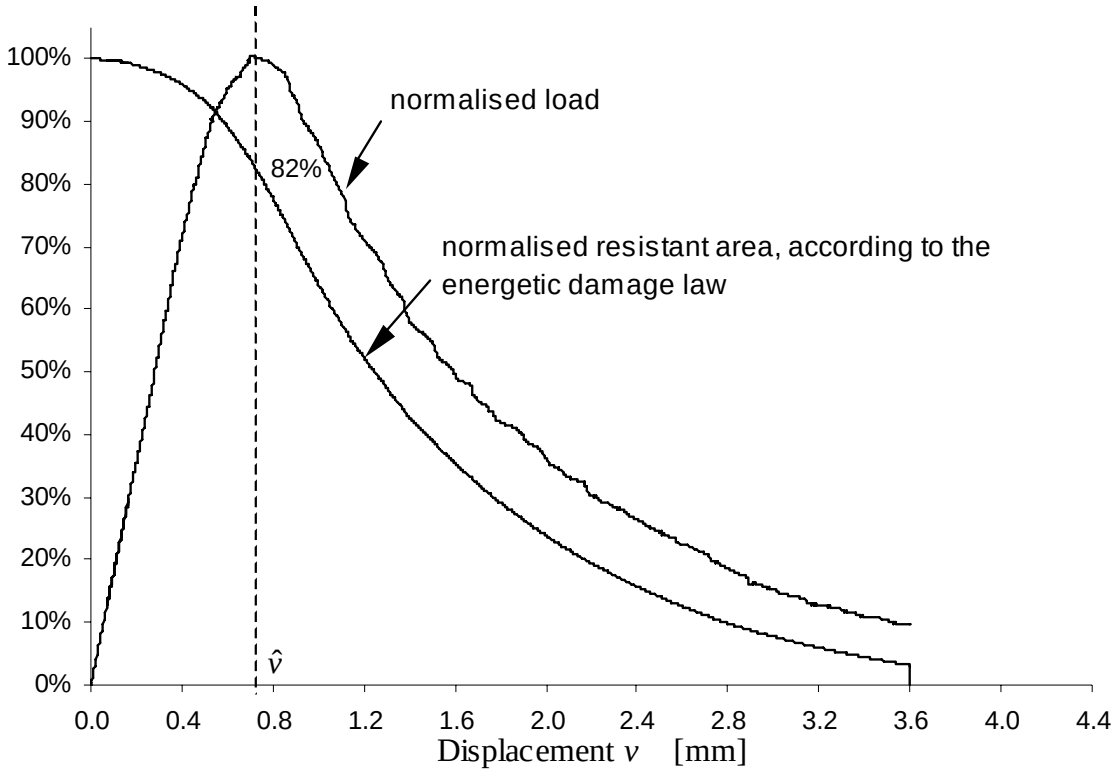
100%
90%
80%
70%
60%
50%
40%
30%
20%
10%
0%
normalised load
82%
normalised resistant area, according to the
energetic damage law
$\hat{v}$
0.0
0.4
0.8
1.2
1.6
2.0
2.4
2.8
3.2
3.6
4.0
4.4
Displacement v [mm]

Fig. 9 – Elena Ferretti

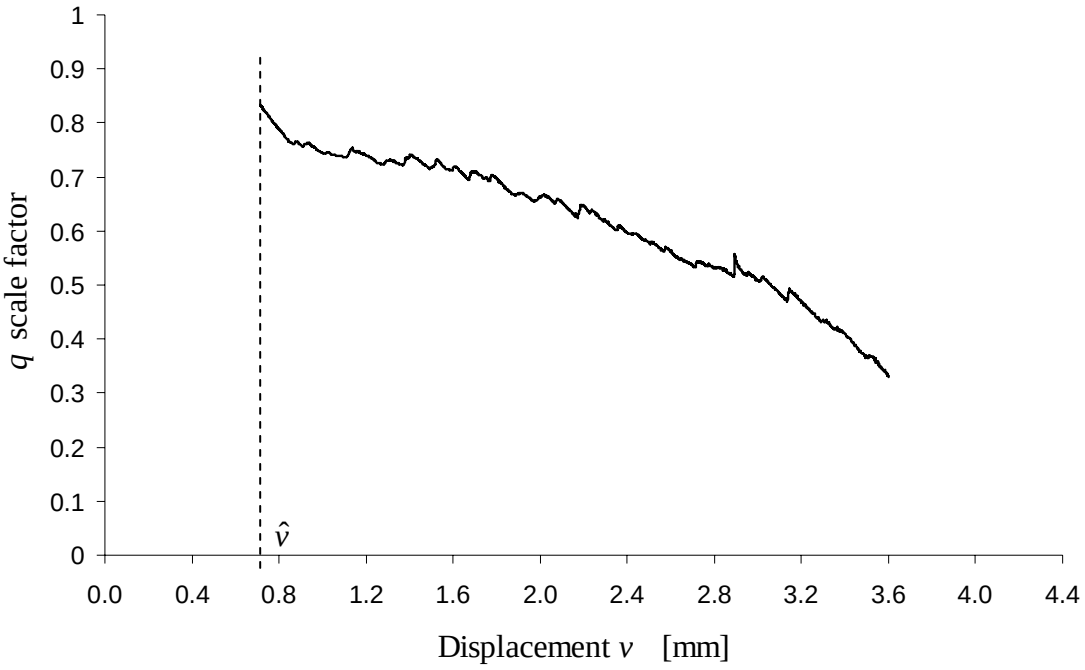
1
0.9
0.8
0.7
0.6
0.5
0.4
0.3
0.2
0.1
0
q scale factor
$\hat{v}$
0.0
0.4
0.8
1.2
1.6
2.0
2.4
2.8
3.2
3.6
4.0
4.4
Displacement v [mm]

Fig. 10 – Elena Ferretti

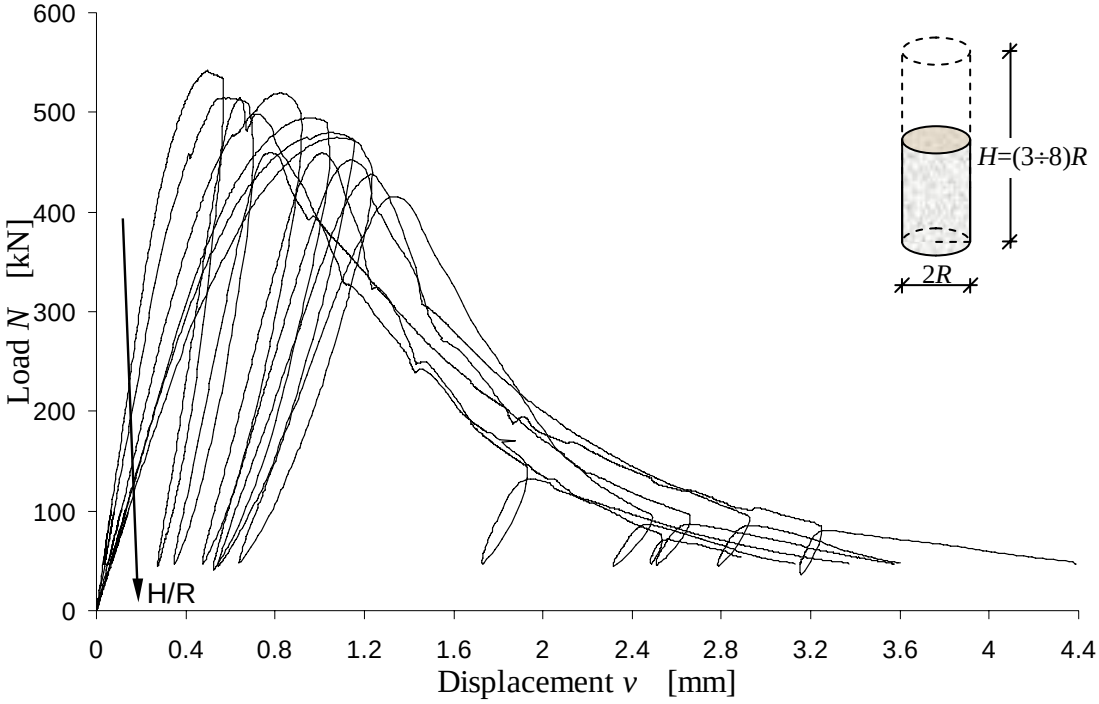
600
500
400
300
200
100
0
Load N [kN]
H/R
0
0.4
0.8
1.2
1.6
2
2.4
2.8
3.2
3.6
4
4.4
Displacement v [mm]
H=(3÷8)R
2R

Fig. 11 – Elena Ferretti

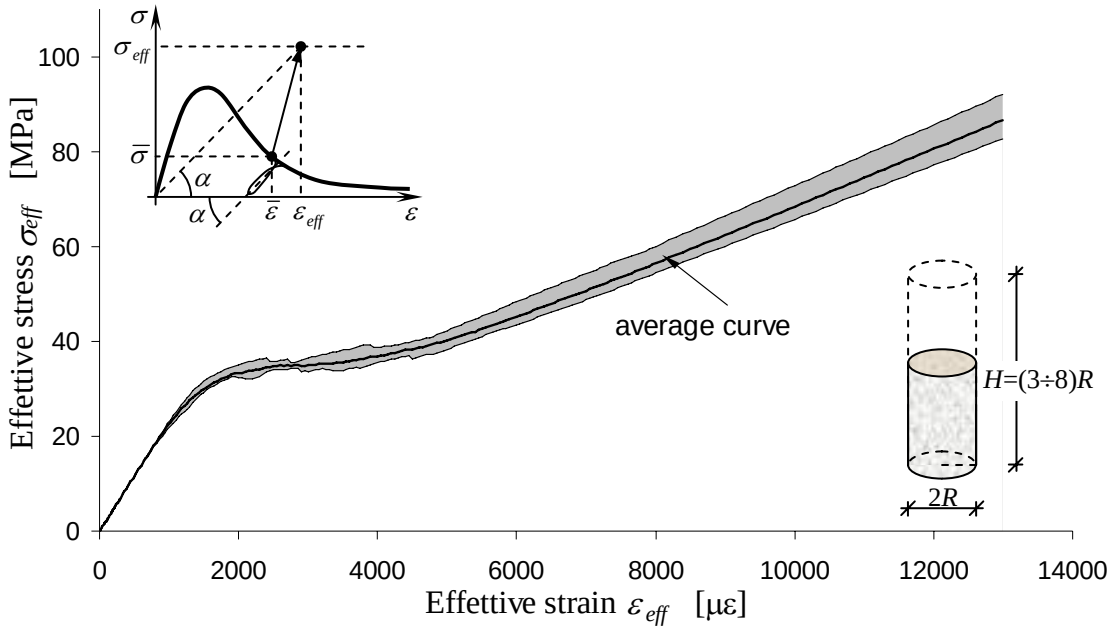
σ
σ_eff
σ̄
α
α
ε̄
ε_eff
ε
Effettive stress σ_eff [MPa]
100
80
60
40
20
0
0
2000
4000
6000
8000
10000
12000
14000
Effettive strain ε_eff [με]
average curve
H=(3÷8)R
2R

Fig. 12 – Elena Ferretti

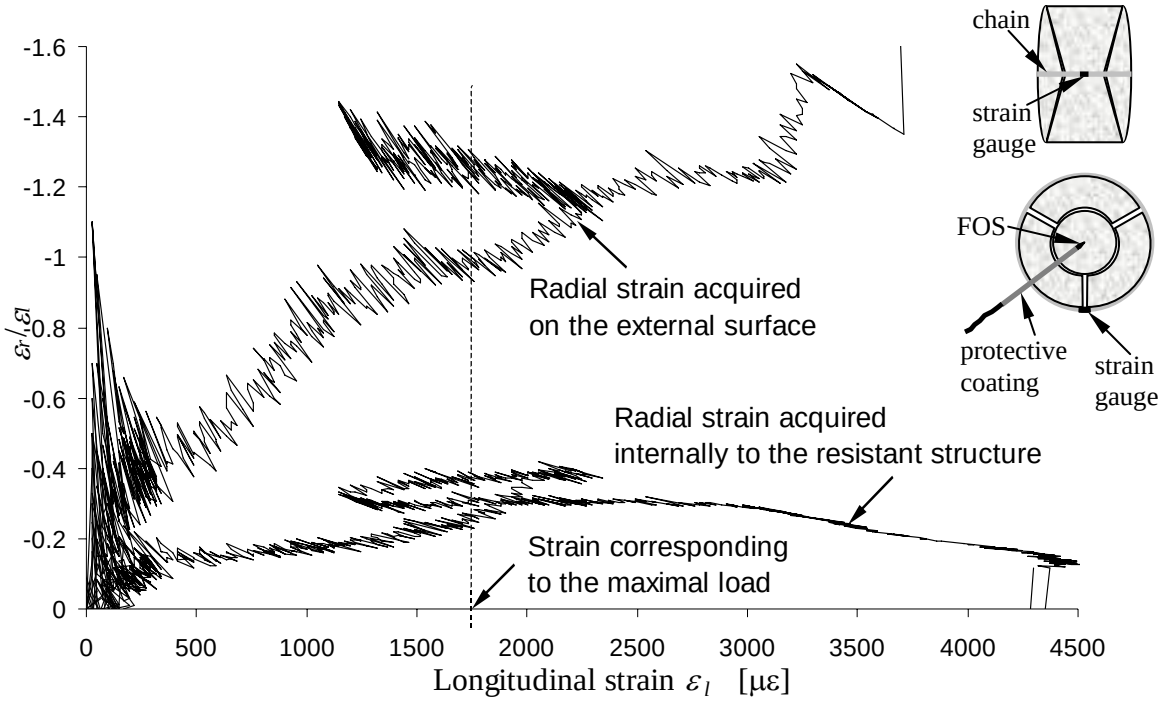
chain
strain gauge
FOS
protective coating
strain gauge
Radial strain acquired on the external surface
Radial strain acquired internally to the resistant structure
Strain corresponding to the maximal load
-1.6
-1.4
-1.2
-1
-0.8
-0.6
-0.4
-0.2
0
0
500
1000
1500
2000
2500
3000
3500
4000
4500
Longitudinal strain ε_l [με]

Fig. 13 – Elena Ferretti

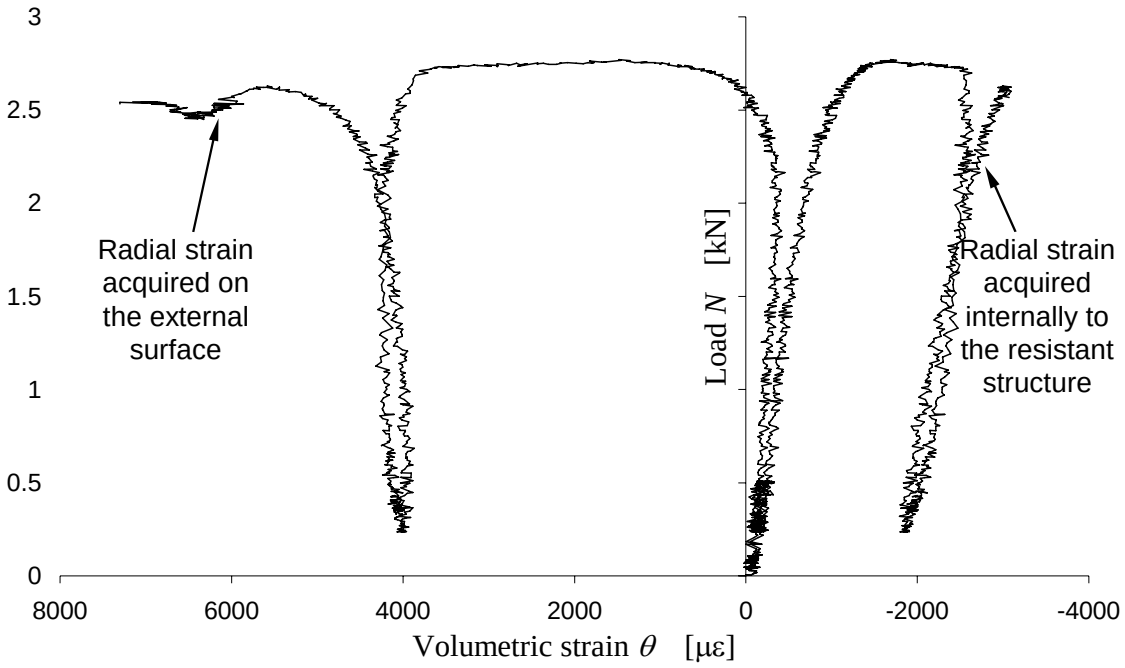
3
2.5
2
1.5
1
0.5
0
8000
6000
4000
2000
0
-2000
-4000
Load N [kN]
Volumetric strain θ [με]
Radial strain acquired on the external surface
Radial strain acquired internally to the resistant structure

Fig. 14 – Elena Ferretti